Late Holocene diatom biostratigraphy and sea-level changes in the southeastern Beaufort Sea

Stéphane Campeau, Arnaud Héquette, and Reinhard Pienitz

Abstract: Late Holocene sediments from the Atkinson Point area were analysed to provide quantitative reconstructions of recent sea-level changes in the southeastern Beaufort Sea. The succession of diatom assemblages in five cores revealed paleoenvironmental changes induced by the transgression of the Beaufort Sea during successive periods of lacustrine conditions, breaching and flooding of thermokarst lakes by the sea, and the landward migration of sandy spits. Based on radiocarbon dates and quantitative paleodepth determinations, a relative sea-level curve for the late Holocene has been developed. Despite a loss of temporal precision due to old carbon contamination, an envelope of sea-level change has been defined for the last 2 ka BP, suggesting a sea-level rise in the order of 1.1 mm a^{-1} for the last millennium. This paper presents the first sea-level reconstruction inferred from a diatom-based transfer function. It represents an improvement over traditional methods which were limited to qualitative estimates of past sea levels.

Résumé: Les sédiments tardi-holocènes de la région de la pointe Atkinson ont été analysés afin de reconstituer quantitativement les variations du niveau marin relatif de la partie sud-est de la mer de Beaufort. Les cinq carottes analysées comportent une séquence transgressive composée à la base de biofaciès de lac de thermokarst surmontés par des biofaciès lagunaires et d'avant-côte. Les paléoprofondeurs inférées par une fonction de transfert, associées à des datations au radiocarbone, ont permis de préciser les taux de relèvement du niveau marin précédemment publiés. Malgré une perte de précision due à la contamination des sédiments datés par du vieux carbone, une courbe de la hausse du niveau marin relatif fut établie pour les deux derniers millénaires, laquelle suggère une hausse probable de 1,1 mm a^{-1} pour le dernier millénaire. Cette étude présente la première reconstitution quantitative des variations du niveau marin effectuée à partir d'une fonction de transfert basée sur les assemblages de diatomées. Elle représente une amélioration par rapport aux procédés traditionnels qui ne fournissaient que des données qualitatives sur la position relative des anciens niveaux marins.

Introduction

Low-lying coastal regions are particularly sensitive to sea-level variations. The southeastern Beaufort Sea coast, which forms part of the Arctic Coastal Plain, has been classified as highly sensitive to a future rise in sea level due to the predominance of ice-rich unconsolidated sediments and widespread thermokarst erosion (Shaw et al. 1998). At the current rate of sea-level rise, the shoreline recession averages more than 1 m a^{-1} with maximum rates exceeding 10 m a^{-1} (Forbes and Frobel 1985; Harper et al. 1985; Héquette and Barnes 1990; Héquette and Ruz 1991). The projected rise in sea level, estimated to reach 0.48 m (Wigley and Raper 1992) or 0.34 m (Titus and Narayanan 1995) by the end of the next century, would hasten the rate at which coastal freshwater lakes are breached and converted into brackish coastal embayments and result in more rapid erosion of ice-rich bluffs (Shaw et al. 1998). In a global warming context, coastal retreat would be further accelerated by the generation of more energetic storm waves (due to a decrease in the extent and duration of sea ice) and enhanced thawing of ice-bonded sediments due to the warming of ground temperature (Harry and Dallimore 1989; Solomon et al. 1994). Coastal erosion and flooding hazards in the Beaufort Sea are of concern for the oil and gas industry, parks development, land resource management, conservation of waterfowl habitat, protection of coastal infrastructure and archeological sites, and problems of coastal property loss at Tuktoyaktuk (Shaw et al. 1998).

Estimation of the magnitude of sea-level change over the last millennium in the Beaufort Sea is necessary to evaluate whether future rise in sea level in this area will occur at the same rate or faster than the projected eustatic rise due to global warming. Vertical land movements occurred in the Beaufort Sea during the late Quaternary as a result of collapsing forebulge and, to a lesser extent, basin subsidence, sediment loading, and consolidation of sediments (Hill et al. 1985). However, as the rate of sea-level rise has not been well defined for the last 3 ka, the present rate of subsidence is unclear. Forbes (1980) suggested that the relative sea level (RSL) of the Beaufort Sea has been rising over the last 15 ka. Hill et al. (1985) reported a number of additional ages and proposed a late Quaternary sea-level curve for the Canadian Beaufort Sea. According to this curve, the RSL rose

Received March 25, 1999. Accepted October 26, 1999.

S. Campeau.[1] Centre d'études nordiques and Department of Geography, Université Laval, QC, G1K 7P4, Canada.
A. Héquette. Department of Geography, Université du Littoral, Dunkerque, France.
R. Pienitz. Centre d'études nordiques and Department of Geography, Université Laval, QC, G1K 7P4, Canada.

[1]Corresponding author (e-mail: campsteph@yahoo.com).

Fig. 1. Location of the southeastern Beaufort Sea.

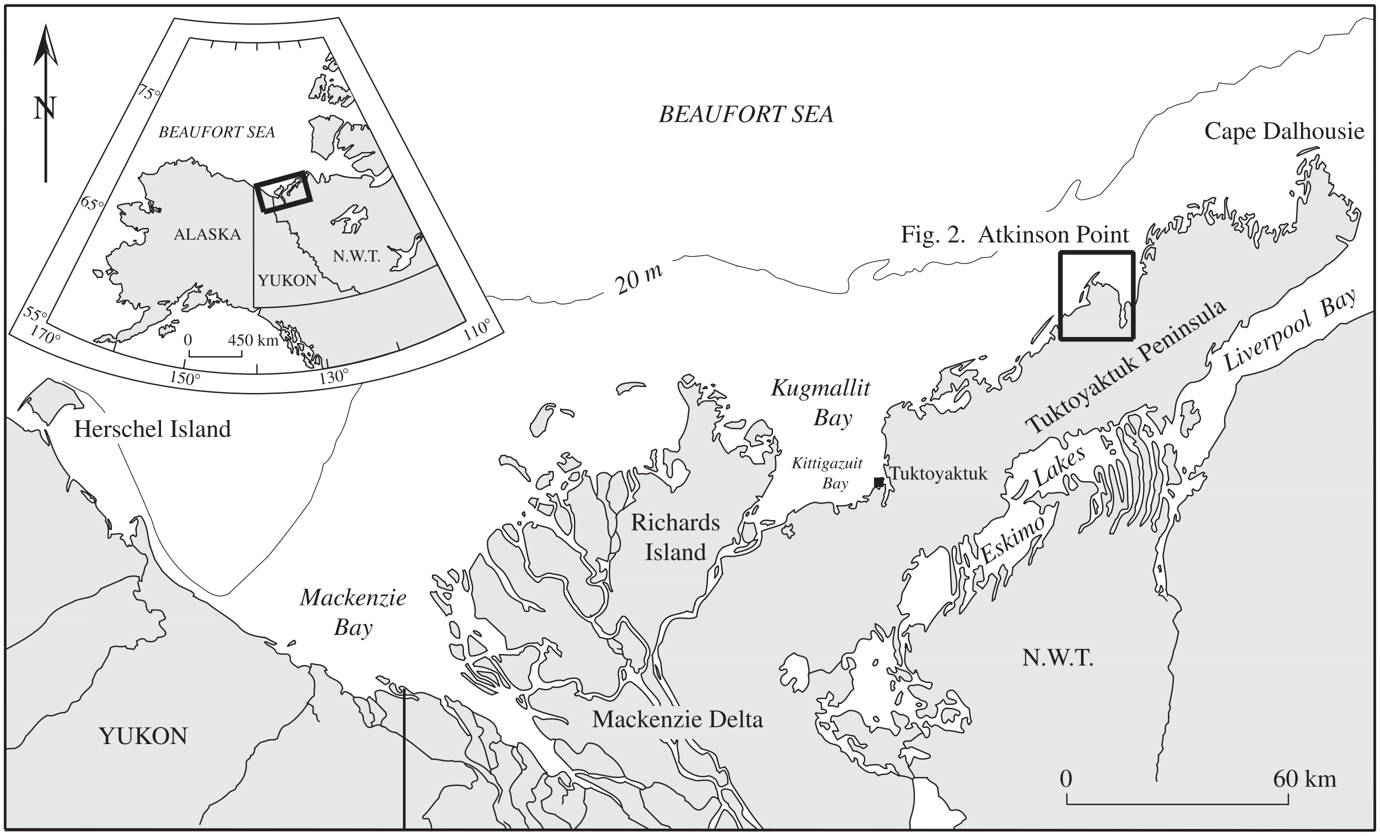

from –140 m at 27 ka BP to a relative highstand of –40 m at approximately 15 ka BP and was then lowered to a Late Wisconsinan lowstand of –70 m. During the Holocene, the RSL rose from –70 m to its present position. The rate of RSL rise during the Holocene was further investigated by Hill et al. (1993). During the early Holocene, this rate was on the order of 4 to 5 mm a^{-1}, and then increased to 7 to 14 mm a^{-1} during the mid-Holocene. Over the last 3 ka, the rate of RSL rise has slowed markedly. Recent radiocarbon dates on peats from modern coastal marshes on the Tuktoyaktuk Peninsula also suggest a slow rise in sea level during the last 1 ka (Hill et al. 1990). Although not statistically significant, tide-gauge data from Tuktoyaktuk indicate that relative mean sea level is still rising at a rate of about 1 mm a^{-1} (Forbes 1980). All these data suggest that the RSL of the Beaufort Sea has risen at a rate between 1 and 4.4 mm a^{-1} during the late Holocene, but more precise data from coastal environments are required to determine what is the exact rate of RSL rise.

This paper reports on a five-core study from the southeastern Beaufort Sea. Besides the analysis of the local paleoenvironmental conditions and the composition of the related diatom assemblages, a paleodepth record was calculated using a diatom-based transfer function. This transfer function was derived from a training set of modern sedimentary environments along the Beaufort Sea coast (Campeau et al. 1999*b*). In the present study, this model is applied to sediment cores from the Atkinson Point area to provide additional insights into the rate of sea-level rise during the late Holocene.

Study area

The Beaufort Sea is the southernmost part of the Arctic Ocean. The southeastern Beaufort Sea is bordered by the Tuktoyaktuk coastlands, which are part of the Arctic Coastal Plain between the Mackenzie Delta and Amundsen Gulf (Rampton 1988) and comprise the Tuktoyaktuk Peninsula and Richards Island (Fig. 1). The southwestern part of the Tuktoyaktuk Peninsula is primarily formed of ice-contact deposits, moraines, or morainal veneer overlain by lacustrine sediments of Holocene age, while the northeastern part consists of glacial outwash sands which are in places covered by eolian or lacustrine sediments (Rampton 1988). The Tuktoyaktuk Peninsula is believed to have been continuously ice free for at least the past 13 ka (Ritchie 1984; Vincent 1989). Between 13 and 8 ka BP, the summer climate was significantly warmer than at present, as a result of an early Holocene Milankovitch insolation maximum (Ritchie et al. 1983; Ritchie 1984). Thermokarst occurs widely on the Tuktoyaktuk coastlands (Rampton 1988; Mackay 1992), as the active layer deepened regionally and numerous retrogressive thaw slumps developed (Rampton 1974). Rampton (1988) suggested that thermokarst basins formed where the deepening active layer intercepted massive icy beds. Ponds formed at such locations and developed into thermokarst lakes as the basins expanded, mainly by retrogressive thaw slumping. At the same time, lake sediment studies in the region showed that from approximately 9 to 5 ka BP, the northern treeline was located 75–100 km north of its present position (Ritchie 1984). Part of the Tuktoyaktuk Peninsula was covered with forest or forest–tundra vegetation. The paleoecological record from lake sites indicated that a gradual climatic cooling began ca. 8 ka BP. The limit of the forests shifted southwards, reaching its present position at about 4.5 ka BP (Spear 1983; Ritchie 1984). Wetlands of the peninsula also responded to the deterioration of climate, with permafrost aggradation at about 6 ka BP and gradual transformation to peatlands by about 5–4.5 ka BP (Vardy et al. 1997). Thermokarst appears to have remained active between 8.5 and 4 ka BP, but with limited development of new thermokarst depressions. As the climate cooled further after 4.5 ka BP (Ritchie 1984), thermokarst activity diminished (Rampton 1974).

The present-day climate of the southern Beaufort Sea coastlands is characterized by short cool summers and long harsh winters. The mean annual temperature at Tuktoyaktuk is –10°C. Precipitation is low, with an annual mean of 142 mm, roughly half of which is accounted for by winter snowfall (Environment Canada 1993). Cold climatic conditions during the Pleistocene have led to the formation of permafrost throughout the region. Permafrost is widespread beneath land areas, ranging from 200 to 500 m in thickness on the Tuktoyaktuk Peninsula, and over 700 m on Richards Island (Judge et al. 1987). Much of the topography in the area can be attributed to the presence of subsurface ground ice. Thermokarst lakes cover about 35% of Richards Island and the Tuktoyaktuk Peninsula, and nearly 70% of the northeastern part of the peninsula.

The coastal areas of the Tuktoyaktuk Peninsula are generally low lying with local relief less than 30 m. The coast consists mainly of bluffs, developed in ice-bonded Quaternary sediments, and of barrier islands and spits, enclosing, partially or completely, lagoons and embayments formed by the breaching of thermokarst lakes. Spits and barrier islands form approximately 30% of the length of the coastline east of the Mackenzie Delta (Harper 1990). Héquette and Ruz (1991) calculated that barrier islands migrate onshore at a mean rate of 3.1 m a^{-1} while spits are retreating at an average rate of 1.7 m a^{-1}. Causes of the widespread coastal retreat along the southeastern Beaufort Sea include (1) wave-induced erosion, (2) thermal erosion (Harper 1990), and (3) the ongoing relative sea-level rise (Hill et al. 1993). The Canadian Beaufort Shelf extends offshore to 60–100 m water depth and is characterized by a very gentle gradient. The area is divided into three distinct physiographic regions: the narrow western shelf adjacent to the United States border, the Mackenzie Trough, and the broad eastern shelf. The fine surficial sediments (silts and clays) of the inner shelf are mainly derived from deposition of suspended sediments from the Mackenzie River.

The coastal ice regime is marked by four "seasons": open water, freezeup, winter and breakup. Coastal ice forms and becomes intermittently stationary during the freezeup season, usually from October to mid-December. The winter season, usually from mid-January through May, is characterized by stable coastal ice (fast ice). The breakup season from June to mid-July is associated with deterioration of the fast ice. This period is followed by the open-water season, from mid-July to early October. During the open-water season, winds originate mainly from the east, southeast, and northwest quadrants. Storm winds (>40 km h^{-1}) are usually from the northwest. The presence of sea ice, during eight to nine months, limits wave activity during most of the year and, even during the open-water season, wave generation is limited by the fetch-restricting pack ice. As a result, the Beaufort Sea is a moderate wave-energy environment and nearly 80% of deep-water waves are less than 1 m in height (Harper and Penland 1982). Tidal range is small, with typical ranges of 0.3 m for neap tides and 0.5 m for spring tides. Storm surges, however, are known to be significant. Surveys of log debris lines stranded on the tundra during these storm events indicate surge elevations up to 2.4 m above mean sea level in the Tuktoyaktuk area (Harper et al. 1988).

The Tuktoyaktuk coastlands are covered by low Arctic tundra vegetation. Upland sites are dominated by dwarf shrubs and lichens, whereas poorly drained peaty areas show ice-wedge polygon and frost hummock development with dominance by *Eriophorum vaginatum* and *Carex* stands (Corns 1974). Sedge tussock flats occur around many lakes, on the bottom of drained lakes, and along coastal lowlands (Mackay 1963).

Methods

Coring

Five cores were collected in the Atkinson Point area along the Tuktoyaktuk Peninsula (Fig. 2) in 1992 and 1993. Coring operations were conducted from an inflatable boat, except for core H-93-7 which was retrieved from a sandy spit. A Livingston coring system was utilized in breached lake basins where sediments were unbonded, soft, and organic (cores C-92-16, C-93-8, C-93-13). A portable vibracoring system was used on the shoreface where sediments were unbonded and firmer than could be penetrated by the Livingston system (core C-92-11). The water depth at each of these coring sites was measured with a 200 kHz depth recorder (Raytheon Fathometer®). The ice-bonded material of a sand spit was collected in springtime using a CRREL auger system with a Stihl power head mounted on a Winke Unipress drill stand (core H-93-7). Sediment subsamples 1 cm thick were taken from cores at the boundaries of lithological units and at varying intervals for diatom and sedimentological analysis. Grain size analyses were done by standard sieving techniques. Organic matter contents were obtained by loss on ignition (550°C for 2 h).

Cleaning and counting

In the Paleoecology laboratory at Laval University, each subsample was digested with acid (30% H_2O_2). The siliceous material was then repeatedly washed and decanted to remove acids. Coarse sand was removed by decanting. An aliquot of the resulting slurry was evaporated onto coverslips, which were subsequently mounted onto glass slides with Naphrax®. Diatoms were identified and enumerated along transects using a Leica DMRB microscope under

Fig. 2. The Atkinson Point area and location of coring sites.

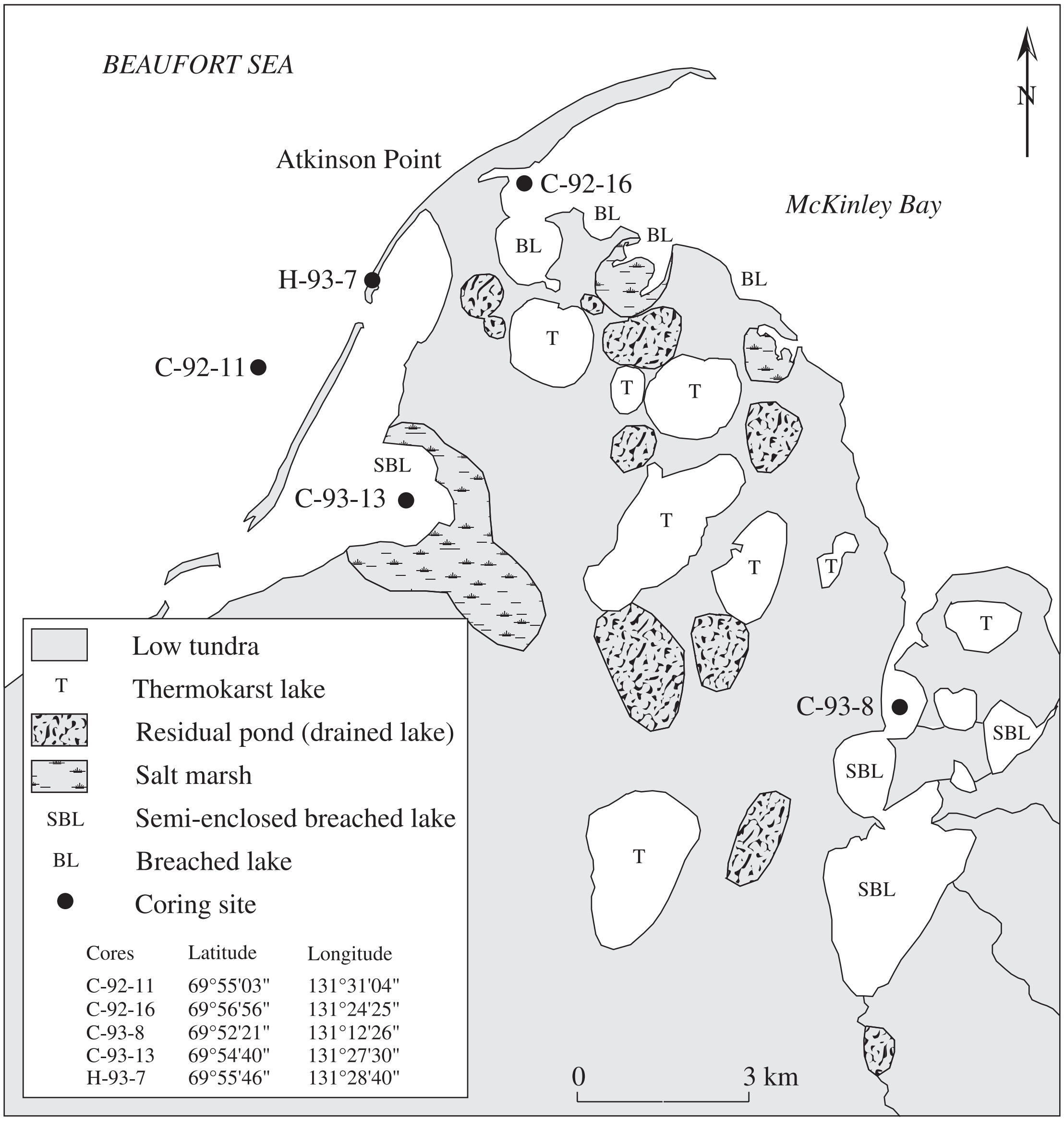

phase contrast illumination at a magnification of 1000×. When possible, 200–300 valves were counted per sample. Broken valves, consisting of more than half of the valves, were counted as one valve. Diatom identifications were made to the lowest taxonomic level possible. The results of diatom analysis have been synthesized in the form of percentage diagrams. The ecology (salinity preferences and life-forms) and taxonomy presented in diagrams are based on marine and freshwater floras. We referred mainly to the following floras: Schmidt et al. (1874–1959), Hustedt (1930, 1953, 1959, 1961–66) in combination with Simonsen (1987), Brockmann (1950), Cleve-Euler (1951–55), van der Werff and Huls (1957–74), Hendey (1964), Patrick and Reimer (1966), Mölder and Tynni (1967–73), Tynni (1975–80), Pankow (1976), Foged (1981), Germain (1981) and Krammer and Lange-Bertalot (1986, 1988, 1991*a*, *b*). Publications on the diatom flora of brackish waters have also provided useful help for identification, especially the works of Poulin et al. (1984*a*, *b*, *c*, 1987), Cardinal et al. (1984, 1986), Bérard-Therriault et al. (1986, 1987) and Poulin et al. (1990) from the Gulf of St.-Lawrence (Canada); Snoeijs (1993), Snoeijs and Vilbaste (1994), Snoeijs and Potapova (1995) and Snoeijs and Kasperoviciene (1996) from the Baltic Sea; and Witkowski (1994) from Gdansk Bay (Poland).

Contemporary environments of the southeastern Beaufort Sea coasts

A detailed analysis of the contemporary diatom assemblages associated with modern sedimentary environments of the Beaufort Sea has previously been conducted by Campeau et al. (1998). Surface sediment assemblages from 74 stations along the coast were analysed to provide modern analogues for future stratigraphic studies. The modern environments sampled are believed to represent the full range of sedimentary facies that may have been preserved in Holocene stratigraphic records of the Beaufort Shelf. Samples were collected from coastal freshwater environments, back-barrier environments, the shoreface, the inner shelf, and the

Mackenzie Delta front area. The fossil assemblages present in sediment cores have been compared with this set of modern samples, in terms of the percentage of the total diatom count per core sample present in both sets, to accurately reconstruct past environments.

Paleodepth inferences

Weighted-averaging (WA) regression was used by Campeau et al. (1999*b*) to develop a water depth inference model based on modern diatom assemblages from the southeastern Beaufort Sea coasts. Surface sediment samples were collected at 74 stations along coasts. Surface grabs or top core sediments were collected. In addition to the measured water depth at each station, the available environmental data consist of some sedimentological data, such as the percentage of sand (≥63 µm), mud (<63 µm) and organic matter, and the distance of the sampling stations from the Mackenzie Delta mouth. All variables had skewed distributions and were log-transformed ($\ln(x+1)$) prior to statistical analyses. In addition, the nine main sedimentary environments occurring in our set of sampling sites, including the freshwater environments (ponds, salt ponds, and coastal peats), salt marshes, semi-enclosed breached lakes, tidal channels, breached lakes and lagoons, shoreface, inner shelf, delta front, and delta front lagoons, were included as dummy (value 0 or 1) passive variables. The relationship between diatom species distribution and water depth was examined using canonical correspondence analysis (CCA) and partial CCA. The water depth accounted for 9.7% of the variance in the data set. WA regression was used to describe the response of diatom species (optima and ranges) as a function of water depth. The optimum water depth of deposition is an estimate of the value along a water-depth gradient at which a taxon achieves its highest abundance relative to other taxa. The optimum of a particular species is estimated by taking the average of all the measured water depths at the stations in which the taxon occurred, weighted by the taxon's relative abundance at each station. Using the computer program WACALIB version 3.3 (Line et al. 1994), WA calibration was performed in the present report based on these species optima to directly infer the position of past relative sea levels from fossil core diatom assemblages. The $\log_e$-inferred water depths were back-transformed to the original unit (m). Core assemblages contained some taxa absent in the modern data set and vice versa. Only taxa present in both sets were included in the analyses, which represent 71.3–96.8% of the total diatom count per core sample. The high similarities between fossil and recent diatom assemblages allowed to produce reliable paleodepth inferences.

Radiocarbon dating

Five samples from the cores were submitted for accelerator mass spectrometry (AMS) dating and standard radiocarbon dating. The submitted samples were composed of organic sediments. According to their diatom assemblages, these sediments were deposited in breached lakes and salt marshes. These levels were selected due to their proximity to an isolation contact and (or) for the reliability of the inferred water depth.

Previous studies have demonstrated that the most reliable radiocarbon ages are those obtained from wood, plant macrofossils, marine shells, and foraminifera (e.g., Short et al. 1994). Total organic carbon dates on both marine and lacustrine sediments with low organic carbon content are usually regarded as unreliable (Fillon et al. 1981). However, due to the lack of more reliable material, all the material selected in this study for radiocarbon dating is composed of organic sediments. The $\delta^{13}C$ values of the dated material were used to evaluate the source of the carbon. As C_3 type plants dominate in the Arctic, terrestrial plants produce $\delta^{13}C$ values of –26 to –30‰ (Stuiver 1975; Peterson et al. 1986; Michel et al. 1989), whereas Arctic algae produce values close to –20‰ (Schell 1983). The $\delta^{13}C$ values associated with the dated core samples, ranging from –27.1 to –36.1, suggested that terrestrial organic matter was the dominant carbon source for these sediments. It is therefore likely that the radiocarbon dates obtained from the cores yielded ages that are older than the age of deposition as a consequence of old terrestrial carbon being washed into lagoons by bank collapse and slumping of tundra peat and dead vegetation. These processes are very active along the Tuktoyaktuk Peninsula coasts, where coastal retreat rates in excess of 1 m a^{-1} are common. Such contamination by old carbon has previously been reported in the Beaufort Sea area (Forbes 1980; Hill et al. 1993) and in other coastal areas (e.g., Zong and Tooley 1996).

To quantify the effect of old carbon contamination and eventually correct the ^{14}C ages, we submitted surface lagoonal sediments (surface grabs) for conventional radiocarbon dating. One would expect to get a recent age for the surface lagoonal sediments, assuming that the organisms living in this material grew in situ, reflecting atmospheric radiocarbon content. However, the results of ^{14}C dating on the top 5 cm of lagoonal surface sediments at two sampling sites in the Atkinson Point area yielded ages of 2890 ± 110 BP (UL-1763) and 4400 ± 90 BP (UL-1762), clearly indicating contamination by old terrestrial carbon. This suggests that all dates from core sediments should be corrected. Consequently, the mean value of these dates (3645 BP) has been used to adjust the ^{14}C ages obtained from downcore samples. The range between these dates, including one standard deviation on each side, has been used as an estimate of the error associated with the adjustment (1510 + 110 + 90 = 1710 ÷ 2 = ±855 yrs). The error associated with the corrected ^{14}C ages is thus considerable and will limit the accuracy of the sea-level reconstruction. However, this correction is essential as it provides a more accurate picture regarding the actual age of deposition of autochthonous lagoonal organic carbon.

Results

Diatom zones

Comparison of core diatom assemblages with contemporary assemblages of the Beaufort Sea coast (Campeau et al. 1998) allows identification of five diatom zones, each of them corresponding to a modern analogue

Diatom zone A. This assemblage is largely dominated by oligohalobian-indifferent species such as *Fragilaria pinnata* and its varieties, *F. construens*, *F. brevistriata*, *Amphora pediculus*, and *Achnanthes minutissima*. These benthic species dominate the modern assemblages of thermokarst lakes on the Tuktoyaktuk Peninsula. They may withstand slightly brackish water conditions, which reflects the maritime character of these lakes. Benthic algal growths are favoured by the shallowness of the lakes and the resulting high levels of available light reaching the bottom. On the other hand, the long duration of ice cover and the shallowness of these lakes may be responsible for the lack of planktonic species.

Diatom zone B. This assemblage is characterized by the occurrence of aerophilic species including *Diploneis interrupta*, *Navicula* aff. *margalithii, N. cincta*, and *Caloneis bacillum*. These diatoms are usually accompanied by mesohalobian epipelic and epipsammic taxa. Zone B corresponds to the contemporary salt marsh diatom flora. Salt marshes commonly developed on drained lake shelves along the southeastern Beaufort Sea coasts and are exposed to high tides and storm surges.

Diatom zone C. The most prominent feature of this diatom zone is the dominance of mesohalobian epipsammic diatoms including *Achnanthes delicatula* ssp. *hauckiana*, *A. lemmermannii*, *Opephora* cf. *parva*, *O. olsenii*, *Fragilaria cassubica*, *F. schulzii*, and *Navicula perminuta*. These species, usually accompanied by some epipelic taxa, are characteristic of modern lagoonal assemblages. Along the Tuktoyaktuk Peninsula, lagoonal environments are made of embayments formed by the breaching of thermokarst lakes. As a consequence of the highly variable environmental conditions and the predominance of sandy material, lagoonal assemblages are dominated by euryhaline epipsammic diatoms with broad ecological tolerances. The epipsammon consists of small appressed species or species with very short stalks, which occupy depressions in the surface of sand grains. Such epipsammic taxa occur generally in intertidal environments with pronounced currents and sediment displacement.

Diatom zone D. This zone is exclusively composed of allochthonous diatoms transported from the shoreface to the surface of sand spits by storm waves and surges. This assemblage only contains a few individuals, usually strongly fragmented. The species encountered include *Achnanthes delicatula* ssp. *delicatula*, *Navicula bipustulata*, *Caloneis crassa*, and *Petroneis humerosa*, which are common taxa of shoreface assemblages.

Diatom zone E. The assemblage of zone E is dominated by mesohalobian epipelic diatoms, such as *Caloneis schumanniana*, *Navicula salinarum*, *N. oestrupii*, *N. jamalinensis*, and *Amphora coffeaeformis*. This assemblage is completed by some epipsammic species, in particular *Achnanthes delicatula* ssp. *delicatula*, which is a common diatom of surf zone sediments, and by planktonic species associated with the Mackenzie River plume and common in inner shelf sediments, such as *Aulacoseira islandica*. The occurrence of a few number of epipsammic and planktonic diatoms in assemblages dominated by epipelic taxa is characteristic of contemporary upper shoreface sediments.

Core C-92-11

In core C-92-11, an organic-rich silty sand unit is overlain by a sand deposit (Fig. 3). The lower boundary of the lowermost diatom zone (C) is dominated by mesohalobian diatoms, such as *Diploneis interrupta*, *Petroneis marina*, and *P. humerosa*, and by planktonic oligohalobian species, mainly *Asterionella formosa* and *Aulacoseira alpigena*. Although this assemblage has no analogue in the modern set of coastal environments described by Campeau et al. (1998), the abundance of freshwater planktonic species and the scarcity of epipsammic taxa is indicative of a deep breached lake influenced by influx of water from terrestrial sources. The relatively great water depth (5.7 m) inferred by the WA model, as compared with the typical water depth (1.6 m) of contemporary backbarrier environments, supports this interpretation. The epipsammic taxa increase towards the upper part of zone C, whereas planktonic species decrease. This shift is associated with a lowering of the water depth as inferred by the WA model. The decrease in water depth probably resulted from the infilling of the lagoon by increasingly proximal washover sands as the barrier island (see Fig. 2) migrated landwards during the late Holocene. The transition between zone C and E is marked by an erosive contact. Except for *Achnanthes delicatula* ssp. *delicatula*, zone E shows a decline in epipsammic species and an increase in epipelic taxa. *Petroneis marina* and *P. humerosa*, which were abundant in zone C, are replaced by *Amphora coffeaeformis*, *Caloneis schumanniana*, *Navicula cancellata*, *N. directa* var. *javanica*, and other epipelic diatoms frequently encountered in shoreface environments. This assemblage is completed by some planktonic species, such as *Aulacoseira islandica* and *Stephanodiscus* cf. *rotula*. As mentioned above, the occurrence of a few epipsammic and planktonic diatoms in assemblages dominated by epipelic taxa is a common feature of upper shoreface sediments. This sequence therefore represents a shoreface environment that has transgressed over a backbarrier environment. The dated sample is from the uppermost part of zone C. It provided an age (after correction for old carbon contamination) of 2555 ± 895 BP. This level has been chosen over the lowermost part of the zone, as it is associated with reliable water-depth inferences, which is not the case for the base of the core due to the lack of a modern analogue.

Core C-92-16

The top and bottom sections of Core C-92-16 consist of clean sand with a thin peat layer between 30 and 33 cm and an organic-rich silty sand unit between 33 and 67 cm (Fig. 4). The lowermost diatom zone (A) is composed of freshwater species including *Achnanthes minutissima* and *Fragilaria* spp. which are characteristic taxa of thermokarst lake assemblages. This zone is bounded at the top by a sharp contact with zone C. The occurrence of a number of aerophilic species, such as *Diploneis interrupta* and *Pinnularia* cf. *streptoraphe*, on both sides of the erosional contact suggests that deposition occurred in close proximity to a salt marsh. Salt marsh sediments have probably been eroded during the subsequent marine transgression. In zone C, diatom assemblages show the replacement of oligohalobian taxa by mesohalobian epipsammic species, dominated by *Achnanthes delicatula* ssp. *hauckiana*. According to contemporary assemblages and the water-depth transfer function, this zone is associated with a shallow breached lake with relatively high current velocities. This sequence, therefore, represents a lagoonal environment that has transgressed over a thermokarst lake. The peat layer, barren of diatoms, located between 30 and 33 cm, is interpreted as a block of peat derived from bank collapse. These

Fig. 3. Diatom diagram for core C-92-11. Diatoms are classified according to the Halobian system of Hustedt (1953). The biostratigraphic zones were defined based on a detailed analysis of the contemporary diatom assemblages associated with modern sedimentary environments of the Beaufort Sea (Campeau et al. 1999*a*). Paleodepth values were inferred from a diatom-based transfer function developed by Campeau et al. (1999*b*) using weighted-averaging (WA) regression and calibration.

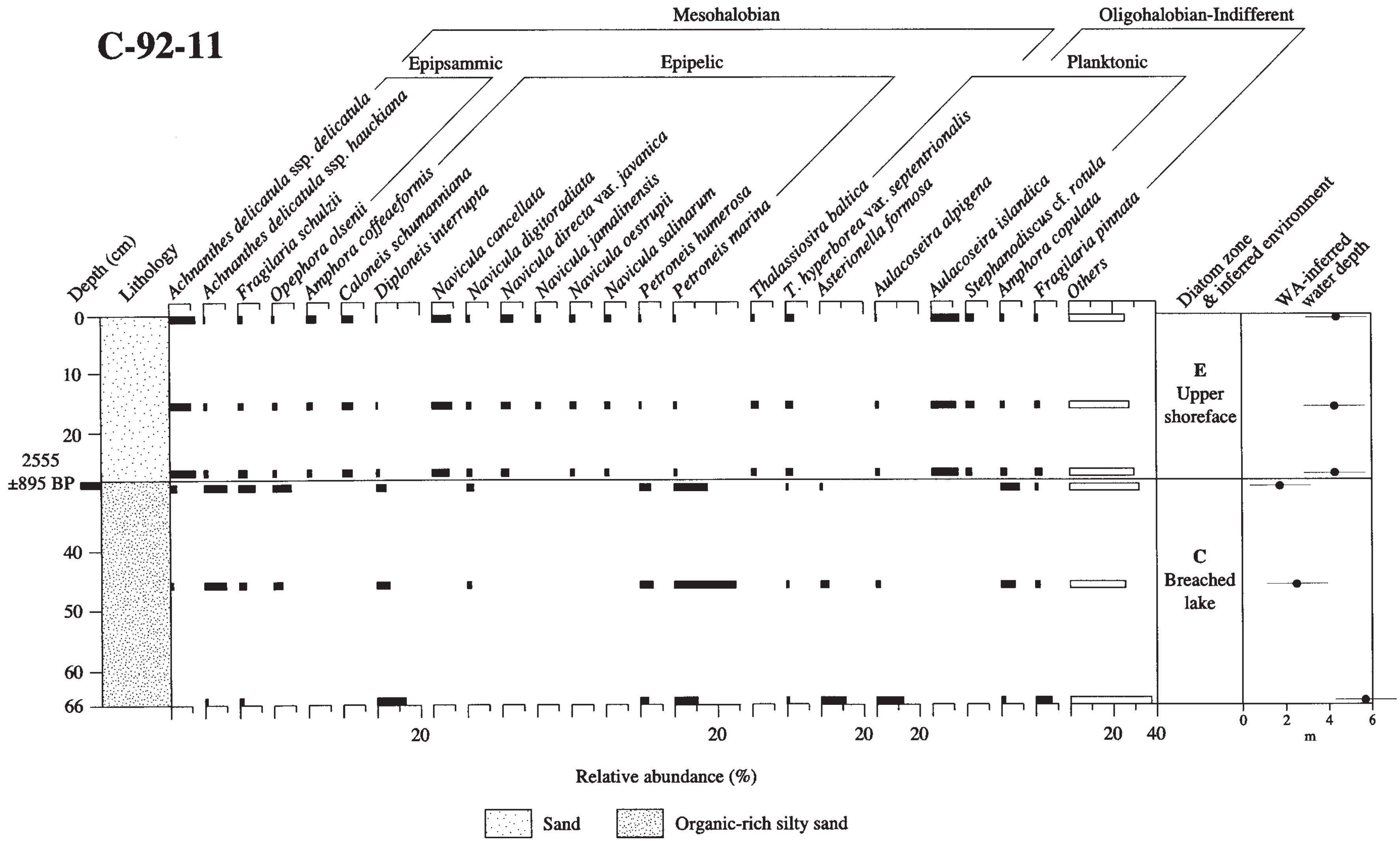

Fig. 4. Diatom diagram for core C-92-16. See Fig. 3 for explanations.

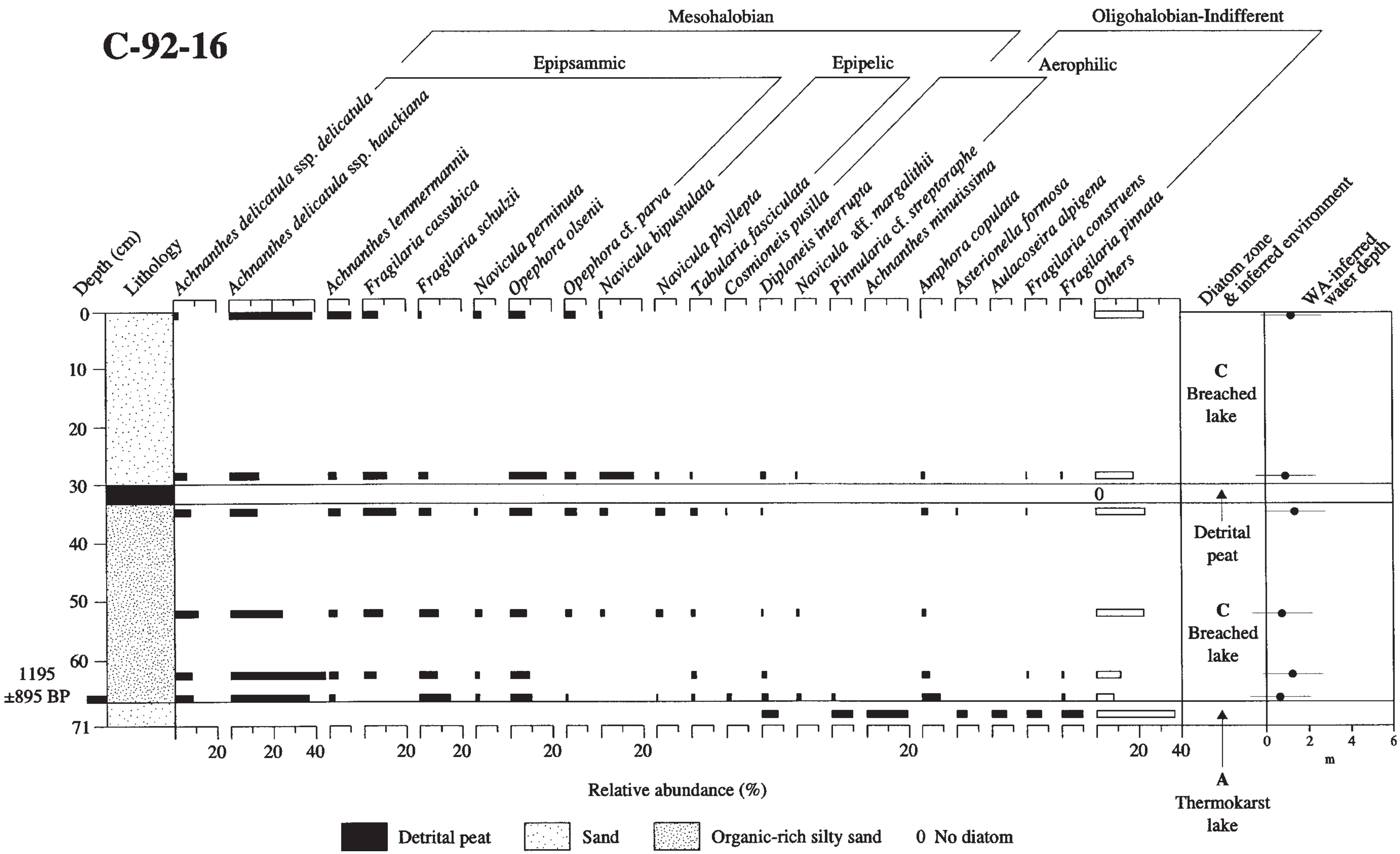

Fig. 5. Diatom diagram for core C-93-8. See Fig. 3 for explanations.

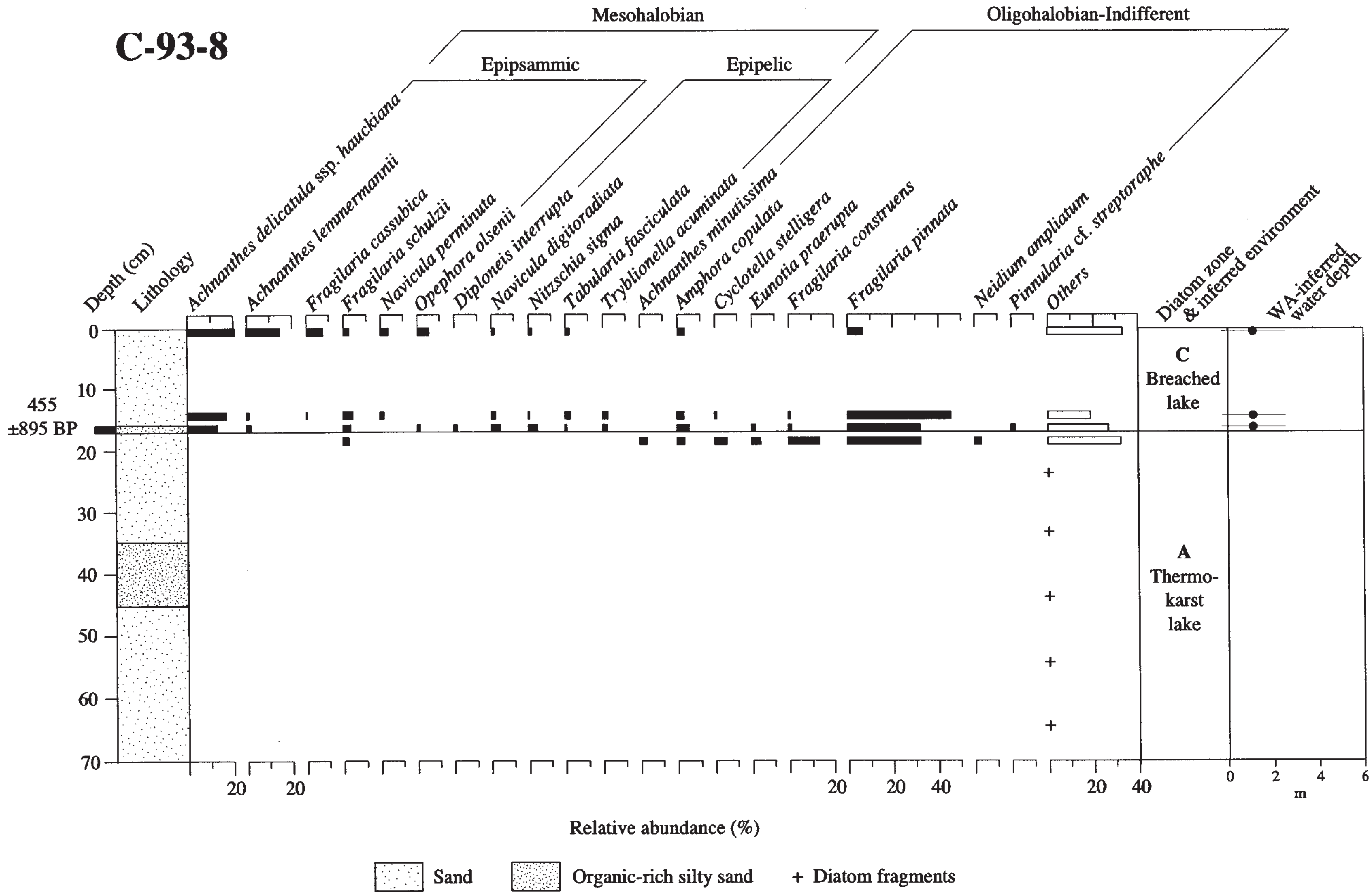

blocks occur in great numbers in present-day lagoonal foreshore sediments. The dated sample is from the lowermost part of zone C and provided an age (after correction) of 1195 ± 895 BP.

Core C-93-8

Core C-93-8 consists of clean sand with organic-rich silty sand layers at 16–17 cm and 35–45 cm (Fig. 5). The lowermost diatom zone (A) contains only fragments of freshwater diatoms. The scarcity of diatoms may be indicative of a sandy shallow nearshore shelf of a thermokarst lake. These shelves surround the central deeper basins of thermokarst lakes and are usually free of diatoms (Campeau et al. 1998). This may be the result of a number of factors, such as the constant reworking of nearshore bottom sediments by waves, wind-driven currents and ice-scouring. The upper boundary of zone A contains well preserved *Fragilaria* species and other freshwater taxa. This zone is bounded at the top by a sharp contact with zone C. The latter is marked by the appearance of mesohalobian species, dominated by *Achnanthes delicatula* ssp. *hauckiana*, and a decline in freshwater diatoms, except for *Fragilaria pinnata* which remains the most abundant species. The occurrence of epipsammic taxa and the abundance of *Fragilaria pinnata* are indicative of a shallow breached lake influenced by freshwater inputs from the land. Subsequently, the record shows a reduced abundance of freshwater diatoms and an increase in epipsammic taxa. This suggests increasing marine influence and higher current velocities towards the top of the core. Thus, this sequence seems to represent a lagoonal environment that has transgressed over a thermokarst lake. The dated sample is from the lowermost part of zone C and provided an age (after correction) of 455 ± 895 BP.

Core C-93-13

The base of core C-93-13 consists of an organic-rich silty sand layer overlain by muddy peat (Fig. 6). The middle section of the core is composed of organic-rich silty sand between 66 and 72 cm, followed by a clean sand layer at 59–66 cm. The uppermost zone of the core consists of muddy peat. The lowermost diatom zone (A) is dominated by *Fragilaria* spp. characteristic of thermokarst lake assemblages. The lower boundary of this zone contains only fragments of freshwater diatoms. This layer may represent the initial phase of the lake. The transition between zones A and B is marked by a gradual contact, as all the freshwater species occurring in zone A are also present in zone B. The lower boundary of zone B is distinguished by the appearance of epipsammic and aerophilic species, the latter including *Diploneis interrupta*, *Navicula eidrigiana*, *N.* aff. *margalithii*, and *Caloneis bacillum*, which are characteristic species of salt marsh assemblages. This assemblage indicates that the thermokarst lake has been breached and was periodically, but not frequently, inundated by sea water. The low abundance of epipsammic taxa and the dominance of *Fragilaria* species suggest that the basin was influenced only by high tide levels and storm surges. The upper boundary of zone B shows an increase in episammic and aerophilic taxa, the appearance of epipelic diatoms, and a drastic decline in freshwater species. This indicates that the mean sea level reached the basin. The WA-inferred water depth is close to zero. The abundance of mesohalobian taxa and the drop in oligohalobian species clearly indicate that this assemblage was permanently tidally influenced. The sand layer, between zones B and C, which contains only fragments of mesohalobian diatoms, probably originates from an intensification of sea influence and may be interpreted as a storm deposit. Zone C is marked by an increase in mesohalobian epipsammic species, dominated by *Achnanthes delicatula* ssp. *hauckiana*, and a further decline in freshwater taxa. Although present at the boundary between the sand layer and zone C, aerophilic species decrease upwards, as the water depth increased. This assemblage has been deposited in a breached lake. The entire sedimentary sequence, therefore, represents a lagoonal environment that has transgressed over a thermokarst lake. The dated sample from the uppermost part of zone B provided an age (after correction) of 1915 ± 895 BP, which gives a good indication of the timing of local marine transgression.

H-93-7

Core H-93-7 consists of a clean sand unit underlain by an organic-rich silty sand unit (Fig. 7). The lowermost diatom zone (C) is dominated by species characteristic of breached lake assemblages. A sharp contact separates this zone from zone D, which contains only a few individuals of species commonly found in the shoreface. This core has been retrieved from the surface of a sandy spit. The sequence represents the infilling of a lagoon by the sediments of a migrating spit. The dated sample from the lowermost part of zone C provided an age (after correction) of 1755 ± 925 BP.

Sea-level index points

The overall stratigraphic successions in the five cores are shown in Fig. 8. The cores are positioned relative to the present-day mean sea level. Each of the five dated samples, associated with the water-depth values inferred by the WA model, represents a sea-level index point. The vertical component of each index point (11th column, Table 1), i.e., its indicative meaning (sensu van de Plassche 1986), was calculated by adding the depth of the dated core section to the water depth at the core station, and by subtracting the WA-inferred water depth from this value. As coring was conducted from an inflatable boat (except for core H-93-7) and tidal range is small, the reference datum-level used was the local mean sea level. The vertical error associated with the index points was thus calculated by adding the range of spring tides (±0.25 m) to the error associated with each WA-inferred water depth. In areas with a small tidal range, the magnitude of water-level variations resulting from meteorological conditions may exceed that of tidal fluctuations between spring tides. Such is the case in the Beaufort Sea where storm surges up to 2.4 m have been reported (Harper et al. 1988). However, these sea-level fluctuations had little effects on the measurement of the water depth as field operations were carried out only in fairweather conditions. As sand is little subjected to compaction (over a geologically short period of a few thousand years and at shallow depths; Greensmith and Tucker 1986) and coastal sediments of the

Fig. 6. Diatom diagram for core C-93-13. See Fig. 3 for explanations.

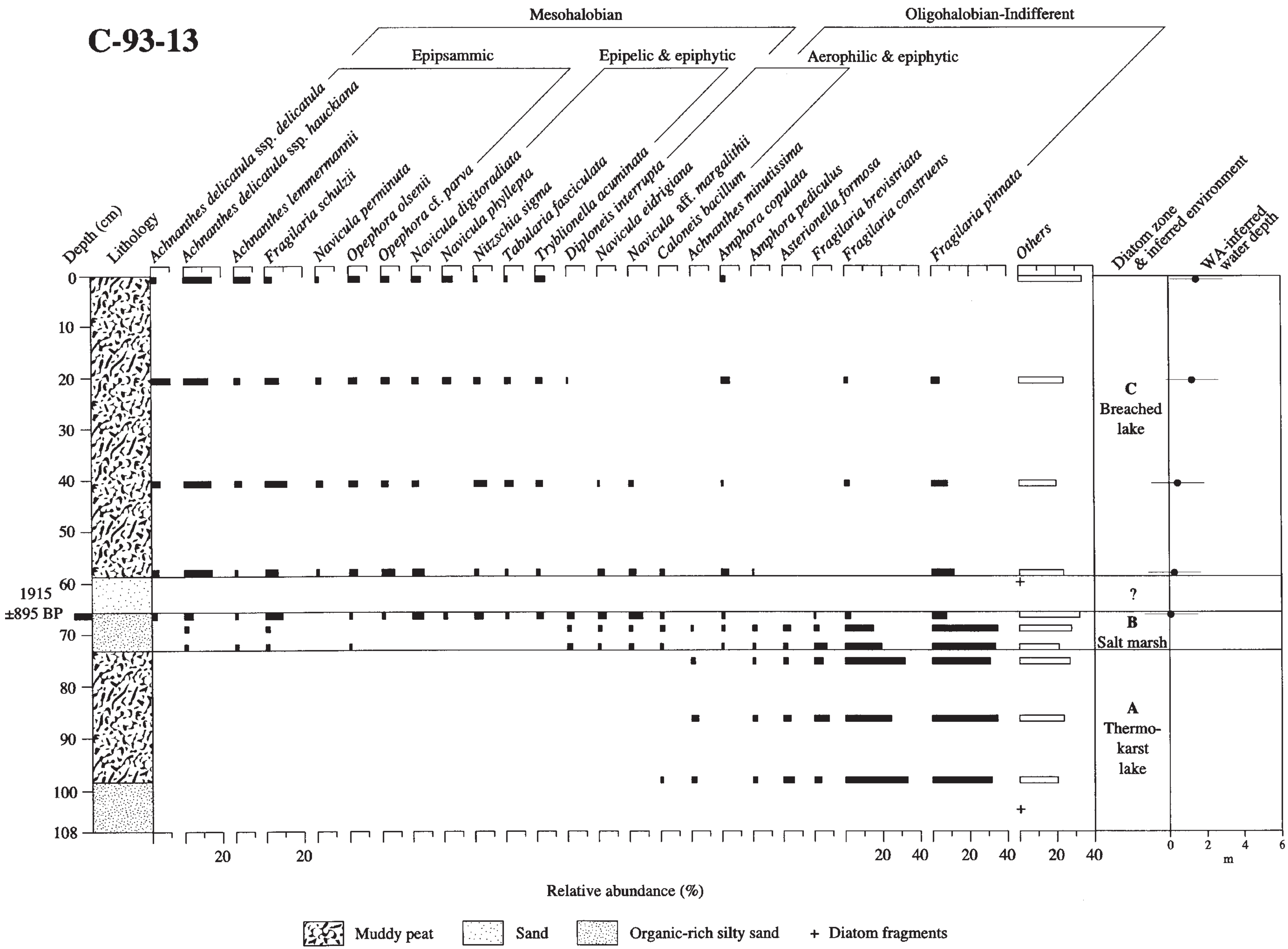

Fig. 7. Diatom diagram for core H-93-7. See Fig. 3 for explanations.

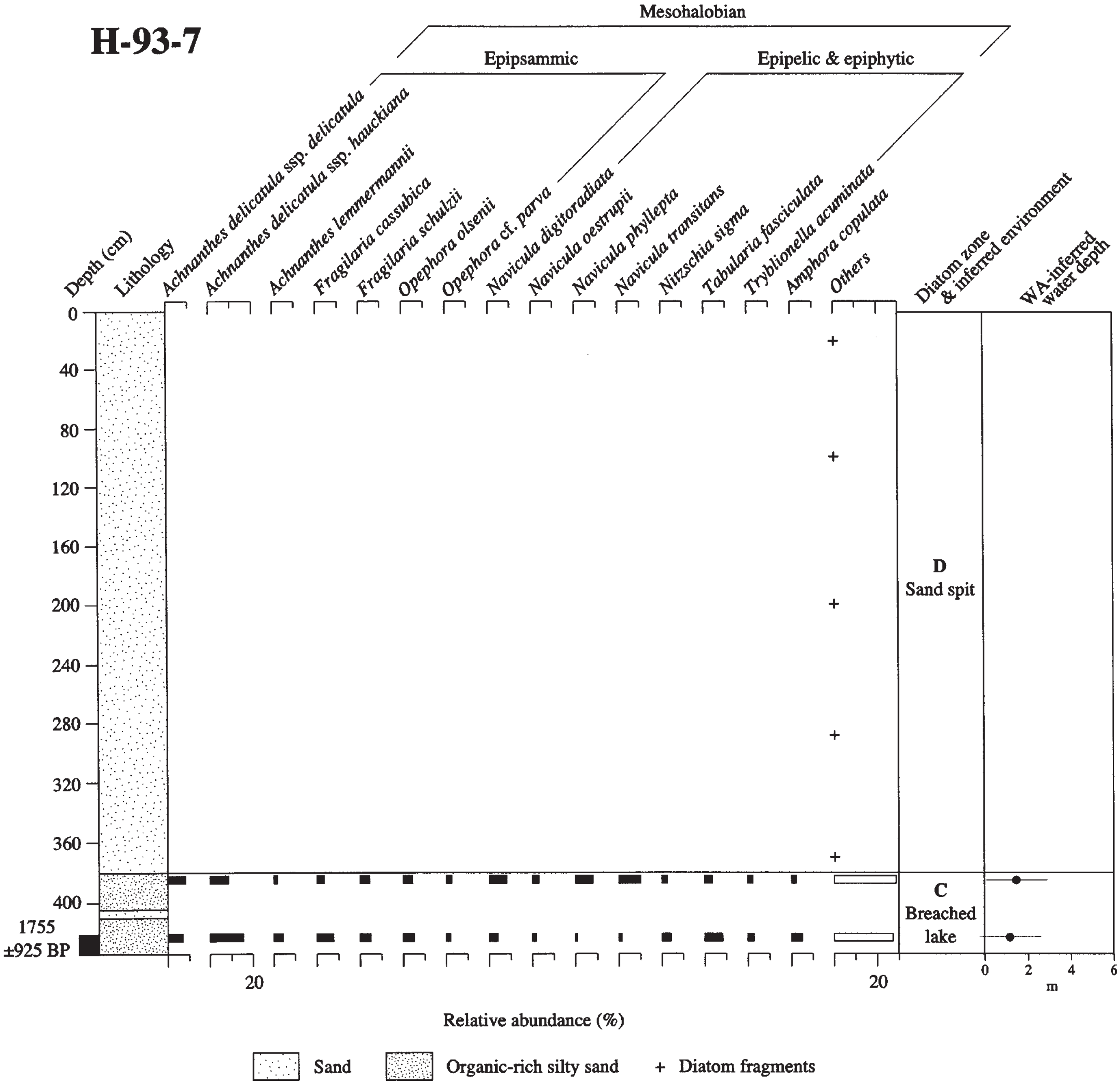

Atkinson Point area rest on clay-deficient Pleistocene sands, no correction was made for sediment compaction.

The horizontal component of each index point (8th column, Table 1) consists of the conventional radiocarbon date corrected for old carbon contamination (–3645 a). The errors associated with these ages have been obtained by adding the standard deviation of the conventional radiocarbon years to half the range (855 a) observed in the radiocarbon ages of lagoonal surface sediments. The age–depth data are plotted in Fig. 9, along with the sea-level data previously published by Forbes (1980) and Hill et al. (1993). A band incorporating the error bars has been drawn, and an estimated curve within the band has been constructed.

Discussion

Relative sea-level change

Despite the relatively large error associated with the corrected radiocarbon ages, the Atkinson index points and the data previously published by Forbes (1980) from the Yukon coast can be used to define an envelope of RSL rise for the last 2 ka BP. The Atkinson index points are direct indicators of sea level, whereas the data from Forbes (1980) indicate that deposition occurred above sea level. According to the estimated curve drawn on Fig. 9, which links the Atkinson index points, the rate of RSL rise was 1.7 mm a^{-1} between 2 ka BP and 1 ka BP. For the last millennium, the estimated

Fig. 8. Overall stratigraphic successions of cores and position of the inferred paleo-sea levels.

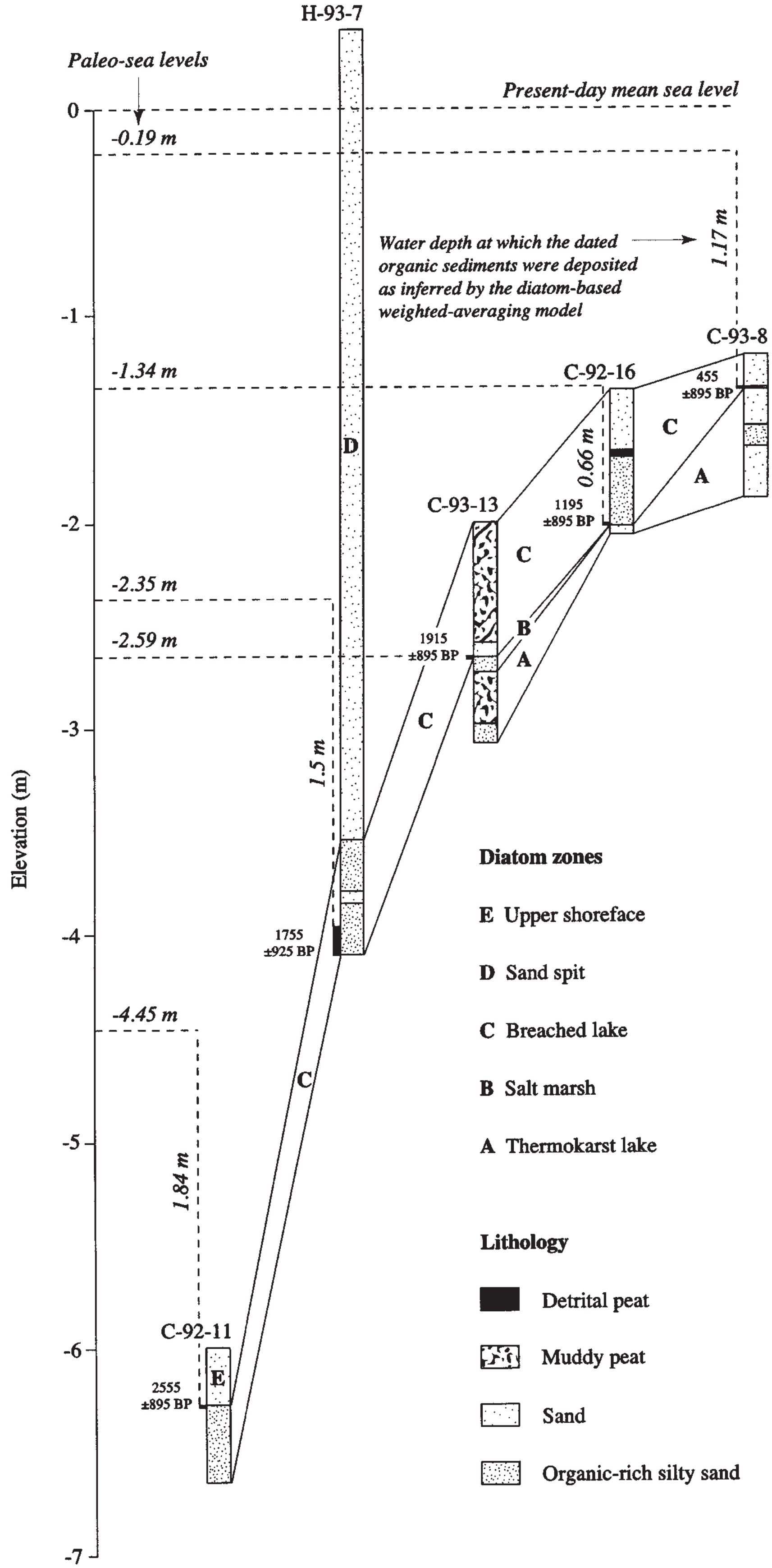

Table 1. Sea-level index points.

Core	Measured water depth at core station (m) ±0.25	Level dated[a] (m)	Material dated	Stratigraphic position	Lab code	Conventional radiocarbon years (±1sd)	Conventional radiocarbon years corrected for old carbon contamination[d] ±(855 + 1sd)	$\delta^{13}C$ (‰)	WA-inferred water depth[e] (m)	Inferred paleo-sea level[f] (m)
C-92-11	6.0	0.29–0.30	Organic sediment	Zone C Top of lagoonal sediment	Beta-110635	6200±40 BP[b]	2555±895 BP	–31.6	1.84±1.42	–4.45±1.67
C-92-16	1.35	0.65–0.66	Organic sediment	Zone C Base of lagoonal sediment	Beta-110636	4840±40 BP[b]	1195±895 BP	–30.0	0.66±1.42	–1.34±1.67
C-93-8	1.2	0.16–0.17	Organic sediment	Zone C Base of lagoonal sediment	Beta-110637	4100±40 BP[b]	455±895 BP	–36.1	1.17±1.42	–0.19±1.67
C-93-13	2.0	0.66–0.67	Organic sediment	Zone B Top of salt marsh sediment	Beta-110638	5560±40 BP[b]	1915±895 BP	–31.9	0.07±1.41	–2.59±1.66
H-93-7	–0.4	4.25–4.38	Organic sediment	Zone C Base of lagoonal sediment	Beta-82037	5400±70 BP[c]	1755±925 BP	–27.1	1.5±1.42	–2.35±1.67

[a]The depth in cores from which organic sediments were collected for dating.
[b]AMS dating.
[c]Standard radiocarbon dating.
[d]The conventional radiocarbon years corrected for old carbon contamination (–3645 years). The errors associated with these ages were obtained by adding the standard deviation of the conventional radiocarbon years to half the range (855 years) observed in the radiocarbon ages of lagoonal surface sediments.
[e]The paleodepth values inferred from a diatom-based transfer function developed by Campeau et al. (1999*b*) using weighted-averaging (WA) regression and calibration.
[f]The inferred paleo-sea levels were obtained as follows (from table): ((Measured water depth at core station + Level dated) – WA-inferred water depth). The error associated with these values was calculated by adding half the value of spring tides (0.25 m) to the error associated with the WA-inferred water depths.

curve follows the maximum side of the error band which is constrained by the "above datum" indicators reported by Forbes (1980). The resulting minimum rate of RSL rise is 1.1 mm a^{-1}. According to the minimum side of the error band, the maximum possible rate of RSL rise for the last millennium is 2.5 mm a^{-1}.

These results are similar to the data previously published by Hill et al. (1993) which suggested that the maximum probable rate was 2.5 mm a^{-1}. However, the actual rate for the last millennium was probably lower. A rise in sea level at the maximum rate implies that all dates would have to be placed on the minimum side of their error bars, which is not probable. For this reason, it is suggested that the most probable rate for the last millennium corresponds to the minimum possible rate (1.1 mm a^{-1}), which follows the estimated curve that links the Atkinson index points. No small-scale oscillations are inferred from the age–altitude data plotted in Fig. 9, and there is no evidence for such oscillations within the litho- and biostratigraphic data either.

This reconstruction should be seen as exploratory at this stage, due to the imprecise time control. To obtain a definite pattern of late Holocene sea-level fluctuations in this area, three improvements over the present data would be needed. First, a better chronological constraint should be placed on the curve by adding radiocarbon dates from shell material. If shell material is lacking, which is common in sediment cores, a series of surficial sediment samples should be dated to yield more accurate rates of old terrestrial carbon input in Arctic lagoonal basins. Such data would allow the calculation of a more reliable correction for old carbon contamination. Secondly, subsidence due to the degradation of permafrost in coastal areas would have to be quantified. As other subsidence processes, such as forebulge collapse, basin subsidence, sediment loading, and consolidation of sediments, have been minor as compared to periods preceding the late Holocene (Hill et al. 1985), degradation of permafrost may be responsible to a great extent for the low RSL rise observed during the last millennium. Thirdly, the late Holocene RSL in the Mackenzie Delta and the western part of the Beaufort Shelf may have risen at different rates than in the Atkinson Point area. This may be due to differential crustal movements, which, although of small amplitude, may have occurred in the eastern, central, and western parts of the shelf. More data are needed to establish separate curves for these three sections of the shelf.

Diatom-based paleodepth inferences

This paper presents the first sea-level reconstruction derived from a diatom-based transfer function. The use of a water-depth transfer function represents an improvement over traditional methods of sea-level reconstructions which usually provided qualitative estimates of past RSL. Traditional approaches mostly relied on the identification and analysis of transgressive and regressive overlaps by analysing stratigraphic boundaries between terrestrial freshwater sediments and marine littoral facies. In these studies, diatom analysis was used to validate sea-level index points by considering changes in the composition of diatom groups of different salinity preferences. This approach was widely used at the interface between fresh and saline environments to identify lake isolation from the sea in areas of land uplift (e.g.,

Fig. 9. Envelope of late Holocene relative sea-level changes in the Canadian Beaufort Sea.

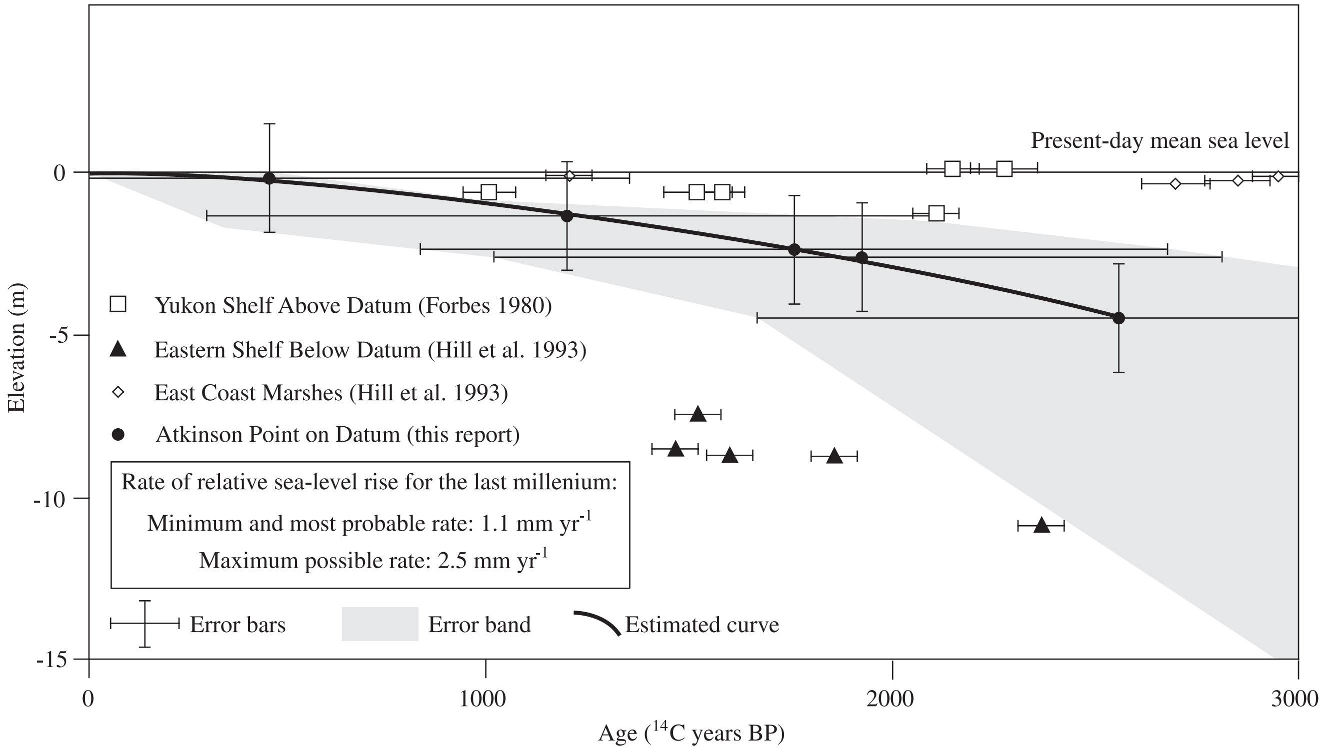

Kjemperud 1986; Stabell 1987; Pienitz et al. 1991), or to indicate marine and brackish water transgressions (e.g., Digerfeldt 1975). Most of these paleo-sea-level reconstructions were constrained by the lack of well-established quantitative relationships between modern diatom assemblages and sea level, and, therefore, none of the index points used were direct sea-level indicators. The radiocarbon dates used in these studies only yielded minimum or maximum ages, depending on which side of the isolation contact they were obtained. Recently, more accurate methods were developed to record the late Holocene rates of sea-level fluctuations. Most of these studies have been conducted in the intertidal zone, especially in salt marshes. The analysis of the altitudinal relationships between contemporary diatom assemblages and water levels in salt marshes allowed more accurate reconstructions of small-scale sea-level changes (e.g., Nelson and Kashima 1993; Shennan et al. 1995, 1996).

None of these methodologies is appropriate for examining the Holocene record of the Beaufort Sea, for two reasons. First, the traditional approach, which consists of identifying isolation contacts, is inappropriate in thermokarst environments. This method requires an accurate evaluation of the lowest sill elevation which controls the occurrence of the first marine influence during a transgression, or the last marine effects during a regression. The former sill elevations of thermokarst lakes cannot be accurately determined as they have been partly eroded by thermo-erosion and by waves and currents during transgression. Furthermore, the first marine influence in a breached lake is likely to occur through salt water intrusions via an outlet channel or an ice-wedge system. In that case, the former sill elevation of the lake is meaningless, and the elevation of the base of the channel cannot be determined precisely. Secondly, the small extent of salt marshes along the southeastern Beaufort Sea coast allows accurate reconstruction of past mean sea levels, but limits their preservation in the sedimentary record. Although salt marshes are very common along the Tuktoyaktuk Peninsula, especially on former lake shelves and in low-lying coastal areas, salt marsh biofacies were absent in most transgressive contacts in the cores, probably as a result of wave and current erosion during transgression. The only salt marsh biofacies identified, however, yielded valuable information on the paleoenvironment. The dated sample from core C-93-13 is believed to yield the most accurate index point as both the paleoenvironment reconstruction and the WA model indicate that deposition occurred close to the mean sea level. In addition, the great floristic similarity observed between fossil and modern salt marsh assemblages and the small vertical extent of the salt marsh zone in core C-93-13 suggest that paleotidal ranges were similar to contemporary ranges.

By determining the relationship between water depth and diatom species distributions and abundances in modern environments, it has been possible to overcome the limitations of traditional approaches and quantitatively infer past relative sea levels. The water-depth model was especially useful in incomplete sequences in which the transition between the lacustrine and marine zones was marked by an erosional contact. In the case of a gradual contact, dating of the lacustrine or the brackish side of an isolation contact represents a good approximation of the first intrusion of salt waters if the sill elevation is known. However, in the case of an erosional contact, part of the sequence is missing and radiocarbon dating will only provide minimum or maximum ages. The water depth transfer function eliminates the need of a freshwater-marine contact. Any section of the brackish-marine sequence may thus be dated and serve as a sea-level index point, as long as datable material is available and water-depth inferences are based on reliable modern analogues. The index points of cores C-92-11 and H-93-7 are good examples of the usefulness of the water-depth transfer function. Since these cores had no lacustrine–marine contact, they could not have provided precise information on the position of paleo-sea levels without using the water-depth model.

Acknowledgements

This project was funded by the Natural Sciences and Engineering Research Council of Canada through a postgraduate scholarship to the senior author and operating grants to A. Héquette and R. Pienitz, and by the Fonds pour la Formation de Chercheurs et l'Aide à la Recherche (Québec). Field work was supported by the Geological Survey of Canada. Further logistic support was provided by the Polar Continental Shelf Project (PCSP) in Tuktoyaktuk. Ron Felix, Michel Cloutier, Marc Desrosiers, Mathieu Avery, and Marie-Pierre Ouellon helped with sample collection. We are grateful to the staff of Centre d'études nordiques at Laval University for their technical support. We also thank the journal reviewers for their helpful comments.

References

Bérard-Therriault, L., Cardinal, A., and Poulin, M. 1986. Les diatomées benthiques de substrats durs des eaux marines et saumâtres du Québec (VI). Naturaliste Cananadien **113**: 405–429.

Bérard-Therriault, L., Cardinal, A., and Poulin, M. 1987. Les diatomées benthiques de substrats durs des eaux marines et saumâtres du Québec (VIII). Naturaliste Cananadien **114**: 81–103.

Brockmann, C. 1950. Die Watt-Diatomeen der Schleswig-holsteinischen Westküste. Abhandl. Senckenberg. Naturforsch. Ges., **478**: 1–76.

Campeau, S., Pienitz, R., and Héquette, A. 1999*a*. Diatoms from the Beaufort Sea coast, southern Arctic Ocean (Canada): Modern analogues for reconstructing Late Quaternary environments and relative sea levels. Bibliotheca Diatomologica, Vol. 42, J. Cramer, Stuttgart.

Campeau, S., Pienitz, R., and Héquette, A. 1999*b*. Diatoms as quantitative paleodepth indicators in coastal areas of the southeastern Beaufort Sea, Arctic Ocean. Palaeogeography, Palaeoclimatology, Palaeoecology **146**: 67–97.

Cardinal, A., Poulin, M., and Bérard-Therriault, L. 1984. Les diatomées benthiques de substrats durs des eaux marines et saumâtres du Québec (IV). Naturaliste Cananadien **111**: 369–394.

Cardinal, A., Poulin, M., and Bérard-Therriault, L. 1986. Les diatomées benthiques de substrats durs des eaux marines et saumâtres du Québec (V). Naturaliste Cananadien **113**: 167–190.

Cleve-Euler, A. 1951–55. Die diatomeen von Schweden und Finnland. Teil III. Kungliga Svenska Vetenskapsakademiens Handlingar. Fjärde Serien, Band 2 (1951), No.1; Band 3 (1952), No. 3; Band 4 (1953), No. 1; Band 4 (1953), No. 5; Band 5 (1955), No.4.

Corns, I.G.W. 1974. Arctic plant communities east of the Mackenzie Delta. Canadian Journal of Botany, **52**: 1731–1745.

Digerfeldt, G. 1975. A standard profile for Litorina transgressions in western Skane, South Sweden. Boreas, **4**: 125–142.

Environment Canada 1993. Canadian climate normals 1961–1990. Vol. 3, Yukon and Northwest Territories. Atmospheric Environment Service.

Fairbanks, R.G. 1989. A 17 000-years glacio-eustatic sea level record: influence of glacial melting rates on the Younger Dryas event and deep-ocean circulation. Nature, **342**: 637–642.

Fillon, R.H., Hardy, I.W., Wagner, F.J.E., Andrews, J.T., and Josenhans, H.W. 1981. Labrador shelf: Shell and total organic matter–14C discrepancies. Geological Survey of Canada, Paper 81–1B, pp. 105–111.

Foged, N. 1981. Diatoms in Alaska. Bibliotheca Phycologica, Band 53. J. Cramer Verlag, Vaduz.

Forbes, D.L. 1980. Late Quaternary sea levels in the southern Beaufort Sea. *In* Current research part B, Geological Survey of Canada, Paper 80–1B, pp. 75–87.

Forbes, D.L., and Frobel, D. 1985. Coastal erosion and sedimentation in the Canadian Beaufort Sea. *In* Current research part B, Geological Survey of Canada, Paper 85–1, pp. 69–80.

Germain, H. 1981. Flore des diatomées des eaux douces et saumâtres. Collection "Faunes et Flores actuelles." Boubée, Paris.

Greensmith, J.T., and Tucker, E.V. 1986. Compaction and consolidation. *In* Sea-level research — a manual for the collection and evaluation of data. *Edited by* O. van de Plassche. Geo Books, Norwich, pp. 591–603.

Harper, J.R. 1990. Morphology of the Canadian Beaufort Sea Coast. Marine Geology, **91**: 75–91.

Harper, J.R., and Penland, P.S. 1982. Beaufort Sea sediment dynamics. Woodward-Clyde Consultants, Victoria, B.C., technical report for the Geological Survey of Canada.

Harper, J.R., Reimer, P.D., and Collins, A.D. 1985. Canadian Beaufort Sea: Physical Shore-Zone Analysis. Geological Survey of Canada, Open File 1689.

Harper, J.R., Henry, R.F., and Stewart, G.G. 1988. Maximum storm surge elevations in the Tuktoyaktuk region of the Canadian Beaufort Sea. Arctic, **41**: 48–52.

Harry, D.G., and Dallimore, S.R. 1989. Permafrost, ground ice and global change in the Beaufort Sea coastlands. Geos **18**: 48–53.

Hendey, I. 1964. An introductory account of the smaller algae of British coastal waters. Part V: Bacillariophyceae. Fish. Investig. Series IV, Ministry of Agriculture Fisheries and Food., Her Majesty's Stationery Office, London.

Héquette, A., and Barnes, P.W. 1990. Coastal retreat and shoreface profile variations in the Canadian Beaufort Sea. Marine Geology, **91**: 113–132.

Héquette, A., and Ruz, M.-H. 1991. Spit and barrier island migration in the southeastern Canadian Beaufort Sea. Journal of Coastal Research, **7**: 677–698.

Hill, P.R., Mudie, P.J., Moran, K., and Blasco, S.M. 1985. A sea-level curve for the Canadian Beaufort Shelf. Canadian Journal of Earth Sciences, **22**: 1383–1393.

Hill, P.R., Héquette, A., Ruz, M.-H., and Jenner, K.A. 1990. Geological Investigations of the Canadian Beaufort Sea Coast. Geological Survey of Canada, Open File.

Hill, P.R., Héquette, A., and Ruz, M.-H. 1993. Holocene sea-level history of the Canadian Beaufort Shelf. Canadian Journal of Earth Sciences, **30**: 103–108.

Hustedt, F. 1930. Die Kieselalgen Deutschlands, Österreichs und der Schweiz unter Berüchsichtigung der übrigen Länder Europas sowie der angrenzenden Meeresgebiete. *In* Kryptogamen-flora von Deutschland, Österreich und der Schweiz. Band 7, Teil 1.

Edited by L. Rabenhorst. Akademische Verlagsgesellschaft, Leipzig.

Hustedt, F. 1953. Die Systematik der Diatomeen in ihren Beziehungen zur Geologie und Ökologie nebst einer Revision des Halobien-systems. Sv. Bot. Tidskr., **47**: 274–344.

Hustedt, F. 1959. Die Kieselalgen Deutschlands, Österreichs und der Schweiz unter Berüchsichtigung der übrigen Länder Europas sowie der angrenzenden Meeresgebiete. *In* Kryptogamen-flora von Deutschland, Österreich und der Schweiz. Band 7, Teil 2. *Edited by* L. Rabenhorst. Akademische Verlagsgesellschaft, Leipzig.

Hustedt, F. 1961–66. Die Kieselalgen Deutschlands, Österreichs und der Schweiz unter Berüchsichtigung der übrigen Länder Europas sowie der angrenzenden Meeresgebiete. *In* Kryptogamen-flora von Deutschland, Österreich und der Schweiz. Band 7, Teil 3. *Edited by* L. Rabenhorst. Akademische Verlagsgesellschaft, Leipzig.

Judge, A.S., Pelletier, B.R., and Norquay, I. 1987. Permafrost base and distribution of gas hydrates. *In* Marine science atlas of the Beaufort Sea—Geology and Geophysics. Geological Survey of Canada, Miscellaneous Report 40, p. 39.

Kjemperud, A. 1986. Late Weichselian and Holocene shoreline displacement in the Trondheimsfjord area, central Norway. Boreas **15**: 61–82.

Krammer, K., and Lange-Bertalot, H. 1986. Bacillariophyceae. 1. Teil: Naviculaceae. *In* Süßwasserflora von Mitteleuropa, Band 2/1. *Edited by* H. Ettl, G. Gärtner, J. Gerloff, H. Heynig, and D. Mollenhauer. Gustav Fisher Verlag, Stuttgart.

Krammer, K., and Lange-Bertalot, H. 1988. Bacillariophyceae. 2. Teil: Bacillariaceae, Epithemiaceae, Surirellaceae. *In* Süßwasserflora von Mitteleuropa, Band 2/2. *Edited by* H. Ettl, G. Gärtner, J. Gerloff, H. Heynig, and D. Mollenhauer. Gustav Fisher Verlag, Stuttgart.

Krammer, K., and Lange-Bertalot, H. 1991a. Bacillariophyceae. 3. Teil: Centrales, Fragilariaceae, Eunotiaceae. *In* Süßwasserflora von Mitteleuropa, Band 2/3. *Edited by* H. Ettl, G. Gärtner, J. Gerloff, H. Heynig, and D. Mollenhauer. Gustav Fisher Verlag, Stuttgart.

Krammer, K., and Lange-Bertalot, H. 1991b. Bacillariophyceae. 2. Teil: Achnanthaceae Kritische Ergänzungen zu Navicula (Lineolatae) und Gomphonema. *In* Süßwasserflora von Mitteleuropa, Band 2/4. *Edited by* H. Ettl, G. Gärtner, J. Gerloff, H. Heynig, and D. Mollenhauer. Gustav Fisher Verlag, Stuttgart.

Line, J.M., ter Braak, C.J.F., and Birks, H.J.B. 1994. WACALIB version 3.3-a computer program to reconstruct environmental variables from fossil assemblages by weighted averaging and to derive sample-specific errors of prediction. Journal of Paleolimnology **10**: 147–152.

Mackay, J.R. 1963. The Mackenzie Delta Area, Northwest Territories, Canada. Department of Mines Technical Survey, Geographical Branch, Memoir 8.

Mackay, J.R. 1992. Lake stability in an ice-rich permafrost environment: examples from the western Arctic coast. *In* Aquatic ecosystems in semi-arid regions: implications for resource management. *Edited by* R.D. Robarts, and M.L. Bothwell. N.H.R.I. Symposium Series 7, Environment Canada, Saskatoon, pp. 1–26.

Michel, F.A., Fritz, P., and Drimmie, R.J. 1989. Evidence of climatic change from oxygen and carbon isotope variations in sediments of a small arctic lake, Canada. Journal of Quaternary Sciences, **4**: 201–209.

Mölder, K., and Tynni, R. 1967–1973. Über Finnlands rezente und subfossile Diatomeen 1–7. Bulletin of the Geological Society of Finland, **39**: 199–217; **40**: 151–170; **41**: 235–251; **42**: 129–144; **43**: 203–220; **44**: 141–159; **45**: 159–179.

Nelson, A.R., and Kashima, K. 1993. Diatom zonation in Southern Oregon tidal marshes relative to vascular plants, foraminifera, and sea level. Journal of Coastal Research., **9**: 673–697.

Pankow, H. 1976. Algenflora der Ostsee. II. Plankton. Gustav Fischer Verlag, Stuttgart.

Patrick, R., and Reimer, C.W. 1966. The diatoms of the United States. Vol. 1: Fragilariaceae, Eunotiaceae, Achnanthaceae, Naviculaceae. Academy of Natural Sciences Philadelphia, Philadelphia.

Peterson, B.J., Hobbie, J.E., and Corliss, T.L. 1986. Carbon flow in a tundra stream ecosystem. Canadian Journal of Fisheries and Aquatic Sciences, **43**: 1259–1270.

Pienitz, R., Lortie, G., and Allard, M. 1991. Isolation of lacustrine basins and marine regression in the Kuujjuaq area, northern Québec, as inferred from diatom analysis. Géographie physique et Quaternaire, **45**: 155–174.

Poulin, M., Bérard-Therriault, L., and Cardinal, A. 1984. Les diatomées benthiques de substrats durs des eaux marines et saumâtres du Québec (I-III). Naturaliste Canadien **111**(*a*): 45–61; (*b*): 275–295; (*c*): 349–367.

Poulin, M., Bérard-Therriault, L., and Cardinal, A. 1987. Les diatomées benthiques de substrats durs des eaux marines et saumâtres du Québec (VII). Naturaliste Canadien **114**: 67–80.

Poulin, M., Bérard-Therriault, L., Cardinal, A., and Hamilton, P.B. 1990. Les diatomées benthiques de substrats durs des eaux marines et saumâtres du Québec (IX). Naturaliste Canadien **117**: 73–101.

Rampton, V.N. 1974. The influence of ground ice and thermokarst upon the geomorphology of the Mackenzie-Beaufort region. *In* Research in polar and alpine geomorphology. *Edited by* B.D. Fahey, and R.D. Thompson. Proceedings of the 3rd Guelph Symposium on Geomorphology, Geo-Abstracts, Norwich, pp. 43–59.

Rampton, V.N. 1988. Quaternary Geology of the Tuktoyaktuk Coastlands, Northwest Territories. Geological Survey of Canada, Memoir 423.

Ritchie, J.C. 1984. Past and present vegetation of the far northwest of Canada. University of Toronto Press, Toronto.

Ritchie, J.C., Cwynar, L.C., and Spear, R.W. 1983. Evidence from northwest Canada for an early Holocene Milankovitch thermal maximum. Nature, **305**: 126–128.

Schell, D.M. 1983. Carbon–13 and carbon–14 abundances in Alaska aquatic organisms: Delayed production from peat in Arctic food webs. Science, **219**: 1068–71.

Schmidt, A. (et al) 1874–1959. Atlas der Diatomaceenkunde. 4 vols. O.R. Reisland, Leipzig.

Shaw, J., Taylor, R.B., Forbes, D.L., Ruz, M.-H., and Solomon, S. 1998. Sensitivity of the coast of Canada to sea-level rise. Geological Survey of Canada, Bulletin 505.

Shennan, I., Innes, J.B., Long, A.J., and Zong, Y.Q. 1995. Holocene relative sea-level changes and coastal vegetation history at Kentra Moss, Argyll, northwest Scotland. Marine Geology **124**: 43–59.

Shennan, I., Long, A.J., Rutherford, M.M., Green, F.M., Innes, J.B., Lloyd, J.M., Zong, Y., and Walker, K.J. 1996. Tidal marsh stratigraphy, sea-level change and large earthquakes 1: A 5000 year record in Washington, USA. Quaternary Science Review **15**: 1023–1059.

Short, S.K., Andrews, J.T., Williams, K.M., Weiner, N.J., and Elias, S.A. 1994. Late Quaternary marine and terrestrial environments, northwestern Baffin Island, Northwest Territories. Géographie physique et Quaternaire, **48**: 85–95.

Simonsen, R. 1987. Atlas and catalogue of the diatom types of Friedrich Hustedt. 3 Vols. J. Cramer, Berlin.

Snoeijs, P. (Editor). 1993. Intercalibration and distribution of diatom species in the Baltic Sea. Vol. 1. Baltic Mar. Biologists Pub. No. 16a, Opulus Press Uppsala.

Snoeijs, P., and Vilbaste, S. (Editors). 1994. Intercalibration and distribution of diatom species in the Baltic Sea. Vol. 2. Baltic Marine Biologists Publication No. 16b, Opulus Press Uppsala.

Snoeijs, P., and Potapova, M. (Editors). 1995. Intercalibration and distribution of diatom species in the Baltic Sea. Vol. 3. Baltic Marine Biologists Publication No. 16c, Opulus Press Uppsala.

Snoeijs, P., and Kasperoviciene, J. (Editors). 1996. Intercalibration and distribution of diatom species in the Baltic Sea. Vol. 4. Baltic Marine Biologists Publication No. 16d, Opulus Press Uppsala.

Solomon, S.M., Forbes, D.L., and Kierstead, B. 1994. Coastal impacts of climate change: Beaufort Sea erosion study. Geological Survey of Canada, Open File 2890.

Spear, R.W. 1983. Paleoecological approches to a study of treeline fluctuations in the Mackenzie Delta region, Northwest Territories: preliminary results. Nordicana, **47**: 61–72.

Stabell, B. 1987. Changes in diatom floras in late Quaternary western and south-eastern Norwegian marine and freshwater sediments: Response to basin isolation from the sea. Nova Hedwigia, **44**: 305–326.

Stuiver, M. 1975. Climate versus changes in C–13 content of the organic component of lake sediments during the Late Quaternary. Quaternary Research, **5**: 251–262.

Titus, J.G., and Narayanan, V.K. 1995. The probability of sea level rise. US Environmental Protection Agency, EPA 230-R-95–008.

Tynni, R. 1975–1980. Über Finnlands rezente und subfossile Diatomeen (8–11). Geological Society of Finland, Bulletin, Vols. 274, 284, 296, 312.

van de Plassche, O. (Editor). 1986. Sea-level research — a manual for the collection and evaluation of data. Geo Books, Norwich.

van der Werff, A., and Huls, H. 1957–1974. Diatomeeënflora van Nederland. Abcoude, Den Haag.

Vardy, S.R., Warner, B.G., and Aravena, R. 1997. Holocene climate effects on the development of a peatland on the Tuktoyaktuk Peninsula, Northwest Territories. Quaternary Research, **47**: 90–104.

Vincent, J.-S. 1989. Quaternary geology of the northern Canadian Interior Plain. *In* Quaternary geology of Canada and Greenland. *Edited by* R.J. Fulton. Geology of Canada, No. 1. Geological Survey of Canada, pp. 100–137.

Wigley, T.M.L., and Raper, S.C.B. 1992. Implications for climate and sea level of revised IPCC emissions scenarios. Nature, **357**: 293–300.

Witkowski, A. 1994. Recent and fossil diatom flora of the Gulf of Gdansk, Southern Baltic Sea: Origine, composition and changes of diatom assemblages during the Holocene. Bibliotheca Diatomologica, Band 28. J. Cramer, Berlin.

Zong, Y.Q., and Tooley, M.J. 1996. Holocene sea-level changes and crustal movements in Morecambe Bay, northwest England. Journal of Quaternary Sciences **11**: 43–58.